COBEM 2021 26th International Congress of Mechanical Engineering
November 22-26, 2021, Virtual Congress, Brazil

COB-2021-0010
ON CONJUGATED HEAT TRANSFER PROBLEMS INVOLVING FILM CONDENSATION IN THE PRESENCE OF A NONCONDENSABLE GAS

Karoline da Costa Rocha Fernandes Ferreira
Laboratory of Thermal Sciences (LATERMO), Mechanical Engineering Department, Universidade Federal Fluminense, UFF
Rua Passo da Pátria 156, bl E, room 206-D, São Domingos, Niterói, Rio de Janeiro, ZIP: 24210-240
fernandeskaroline@id.uff.br

Kleber Marques Lisboa
Laboratory of Thermal Sciences (LATERMO), Mechanical Engineering Department, Universidade Federal Fluminense, UFF
Rua Passo da Pátria 156, bl E, room 206-D, São Domingos, Niterói, Rio de Janeiro, ZIP: 24210-240
kmlisboa@id.uff.br

Abstract. *Full understanding of condensation heat transfer in its many facets has many potential benefits for industrial processes. Since the pioneering Nusselt model for film condensation, many extensions have been accomplished; most notably, the presence of noncondensable gases, even in small concentration, was determinated to severely diminish heat transfer rates and condensate output. In this work, we explore the effect of the coupling between natural convection of an air-water mixture, film condensation in the presence of noncondensables, conduction through a metallic plate, and single-phase convection. For this purpose, the mass, species, and momentum conservation principles are solved under the boundary layer hypothesis using Karman-Pohlhausen's integral method; a simple one-dimensional conduction model is employed for the metallic wall and it is responsible for the coupling of the boundary layer equations stemming from filmwise condensation and single-phase forced convection. The influence of wall materials and main dimensions are investigated with the aim at maximizing the heat transfer rate and, consequently, the condensate productivity. The conjugation effects are shown to be comparable to the ones exacted by the presence of noncondensable gases and ignoring them may be a poorly justifiable decision for many applications. Improvements in the heat transfer rate through the reduction of the conduction thermal resistance stall beyond a certain point in forced-convection-dominated physical situations, indicating that the employment of heat transfer intensification in the channel may be more fruitful.*

Keywords: *Film condensation, noncondensable gases, conjugated heat transfer, boundary layer*

1. INTRODUCTION

Heterogeneous condensation of vapors is induced by thermal contact with a surface whose temperature is sufficiently below the saturation temperature of the condensing substance for the phase change to occur (Collier and Thome, 1994). This physical process is ubiquitous in industry with applications ranging from refrigeration and air-conditioning to nuclear reactor design, among others. Thus, understanding of the mechanisms involved and, consequently, how to properly design condensers (Zhang *et al.*, 2019), heat pipes (Senjaya and Inoue, 2014a, 2014b), desalination equipment (Shahu and Thombre, 2019), etc., either to facilitate or to avoid the occurrence of condensation is crucial.

The study of this phenomenon has led to the identification of two modes of heterogeneous condensation, namely film- and dropwise condensation (Collier and Thome, 1994). Filmwise condensation is characterized by a continuous flow of condensate adjacent to the cold surface, that, once established, ceases the direct contact between the surface and the vapor. On the other hand, in dropwise condensation, a discrete number of droplets form on the cold surface, coalesce, and move, freeing the surface for the nucleation of new droplets. Given a particular condensing substance, say water, whether film- or dropwise condensation will occur depends heavily on the wettability of the surface, with hydrophobic ones favoring the latter (Sharma *et al.*, 2018; El Fil *et al.*, 2020). Regarding heat transfer, one might think at first glance that the presence of a liquid film, with more favorable thermophysical properties, would render filmwise condensation the preferred mode as far as maximizing heat transfer rate is concerned. However, the presence of the film actually adds another thermal resistance to the flow of heat from the bulk vapor to the surface, thereby resulting in lower heat transfer coefficients under these circumstances. Therefore, assuming filmwise condensation is a conservative hypothesis when designing for applications aiming to improve heat transfer, especially considering that dropwise condensation is difficult to maintain during long-term operation (Collier and Thome, 1994).

The presence of noncondensable gases was noted to markedly reduce heat transfer rates associated with condensation on a surface by Othmer (1929), that reported experimental results pointing to a drop by 50% of the heat transfer coefficient with the presence of just 0.5 vol% of air in water vapor, in comparison with results obtained with pure vapor. This fact may be attributed to an accumulation of noncondensable gas at the interface of the condensate, shielding the contact of

water vapor with the liquid and lowering the driving force of heat transfer through the film (Sparrow and Lin, 1964; Minkowycz & Sparrow, 1966). Due to its common presence in several applications (Senjaya and Inoue, 2014a, 2014b; Shahu and Thombre, 2019) and the drastic effect it may have on the performance of the equipment involved, the role of noncondensables in condensation heat transfer and possible interactions with other phenomena is definitely worthy of investigation.

The present work aims to extend the knowledge of condensation heat transfer in the presence of noncondensables to include the effects of conjugation with a solid wall and forced convection inside a channel, as illustrated in Fig. 1. The Karman-Pohlhausen integral method shall be used to solve the governing equations for mass, momentum, and species conservation in the nocondensable gas-vapor mixture. Materials and parameters such as thickness of the wall, and width of the channel are varied to probe their effect on the heat transfer rate and, consequently, in the condensate output.

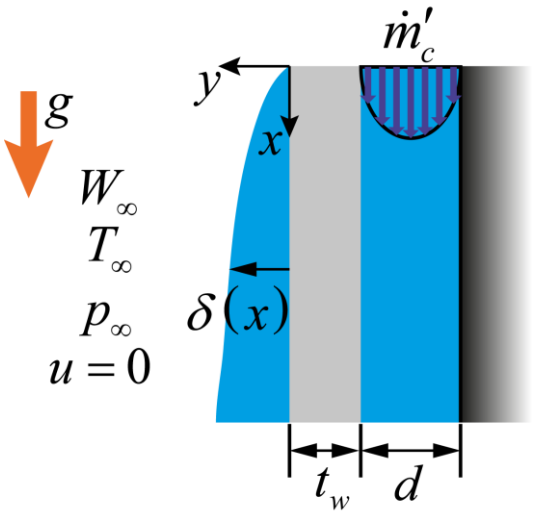

Figure 1. Illustration of the conjugated heat transfer problem involving filmwise condensation.

2. MODEL AND SOLUTION METHODOLOGY

2.1 Forced convection in the channel

Within the channel, the flow is considered to be laminar, hydrodynamically developed, and thermally developing. An average Nusselt number correlation for this physical situation under constant wall heat flux will be employed as follows (Shah and London, 1978),

$$Nu_c = \begin{cases} 1.462L^{*-1/3}, & L^* \leq 0.001 \\ 1.462L^{*-1/3} + 0.589, & 0.001 < L^* < 0.01 \\ 5.385 + \dfrac{0.0238}{L^*}, & L^* \geq 0.01 \end{cases} \tag{1}$$

with,

$$L^* = \frac{L}{D_h Pe_{D_h}} \tag{1}$$

where Nu_c is the Nusselt number in the channel, L is the height of the channel, $D_h = 2d$ is the hydraulic diameter of the channel, Pe_{D_h} is the Péclet number based on the hydraulic diameter. The Nusselt number correlation of eq. (1) was corrected using the ratio between fully developed Nusselt numbers to account for the fact that the rightmost channel wall in Fig. 1 is insulated (Kandlikar *et al.*, 2006).

The heat transfer coefficient can then be obtained as,

$$h_c = Nu_c \frac{k_c}{D_h} \tag{3}$$

where h_c is the average heat transfer coefficient for the forced convection in the channel and k_c is the thermal conductivity of the fluid flowing inside the channel.

Employing an energy balance in an infinitesimal control volume inside the channel and taking into account the wall and condensate film thermal resistances, it is possible to write (Bejan, 2013),

$$\frac{dT_c}{dx} = \frac{2}{\dot{m}'_c c_{p,c}} \left(\frac{t_w}{k_w} + \frac{1}{h_c} + \frac{\delta}{k_l} \right)^{-1} (T_i - T_c) \tag{4}$$

with initial condition given by,

$$T_c(L) = T_{c,e} \tag{5}$$

where T_c is the mean fluid temperature in the channel, T_i is the temperature at the interface between the liquid film and gas mixture, $T_{c,e}$ is the mean fluid temperature at the entrance of the channel, $\dot{m}'_c$ is the mass flow rate per unit of width, $c_{p,c}$ is the specific heat of the fluid in the channel, t_w is the wall thickness, k_w is the thermal conductivity of the wall, k_l is the thermal conductivity of the liquid film, and δ is the liquid film thickness.

2.2 Conduction through the wall

The heat conduction through the wall is considered to be one-dimensional, on the assumption that the thickness of the wall is much smaller than its height. Adding the hypotheses of constant thermal conductivity and absence of internal heat generation, we may write the thermal resistance associated with heat conduction through the wall as,

$$R_w = \frac{t_w}{k_w} \tag{6}$$

where R_w is the thermal resistance through the wall

2.3 Condensate film model

Laminar flow of the liquid film depicted in Fig. 1 with constant thermophysical properties is assumed. Furthermore, the hypotheses of the so-called Nusselt model are adopted, i.e., negligible inertial and convective transport, and axial diffusive transport (Nusselt, 1916). These assumptions are especially accurate when condensation occurs in the presence of noncondensable gases, given the associated reduction in condensate output (Sparrow and Lin, 1964; Minkowycz and Sparrow, 1966). The resulting model is given by,

$$\frac{\partial u_l}{\partial x} + \frac{\partial v_l}{\partial y} = 0 \tag{7}$$

$$v_l \frac{\partial^2 u_l}{\partial y^2} + g = 0 \tag{8}$$

$$k_l \frac{\partial^2 T_l}{\partial y^2} = 0 \tag{9}$$

with boundary conditions,

$$u_l(x,0) = v_l(x,0) = 0 \tag{10}$$

$$\left(\frac{\partial u_l}{\partial y} \right)_{y=\delta} = 0 \tag{11}$$

$$-k_l \left(\frac{\partial T_l}{\partial y} \right)_{y=0} = \left(\frac{t_w}{k_w} + \frac{1}{h_c} \right)^{-1} [T_c(x) - T_l(x,0)] \tag{12}$$

$$T_l(x,\delta) = T_i \tag{13}$$

where u_l is the velocity component in the x-direction, v_l is the velocity component in the y-direction, ν_l is the kinematic viscosity of the liquid film, k_l is the thermal conductivity of the liquid film, g is the acceleration of gravity, and T_l is the temperature field in the liquid film.

In addition, mass and energy balances written for an infinitesimal portion of the liquid film yield,

$$\dot{m}'' = \rho_l \frac{d}{dx} \left\{ \int_0^\delta u_l dy \right\} \tag{14}$$

$$\dot{m}'' h_{fg} = \left(\frac{t_w}{k_w} + \frac{1}{h_c} + \frac{\delta}{k_l}\right)^{-1} (T_i - T_c) \tag{15}$$

where ρ_l is the density of the liquid film, h_{fg} is the latent heat of vaporization of the condensing substance, and $\dot{m}''$ is the condensate mass flux into the liquid film.

Solving eqs. (7-15), we then have,

$$u_l(x,y) = \frac{g\delta^2}{\nu_l}\left[\frac{y}{\delta} - \frac{1}{2}\left(\frac{y}{\delta}\right)^2\right] \tag{16}$$

$$v_l(x,y) = -\frac{g}{2\nu_l} y^2 \delta'(x) \tag{17}$$

$$T_l(x,y) = \frac{k_l(h_c t_w + k_w)T_i + k_w h_c \delta T_c}{k_l(h_c t_w + k_w) + k_w h_c \delta} + \frac{k_w h_c y}{k_l(h_c t_w + k_w) + k_w h_c \delta}(T_i - T_c) \tag{18}$$

$$\dot{m}'' = \frac{\rho_l g}{\nu_l}\delta^2 \delta'(x) \tag{19}$$

$$\frac{\rho_l g h_{fg}}{4\nu_l}\frac{d(\delta^4)}{dx} = \left(\frac{t_w}{k_w \delta} + \frac{1}{h_c \delta} + \frac{1}{k_l}\right)^{-1} (T_i - T_c) \tag{20}$$

2.4 Gas-vapor mixture model

An external natural convection model is proposed to the flow of the mixture between a condensing substance and a noncondensable gas. The Boussinesq approximation shall be adopted, thus considering the density of the mixture constant except in the buoyancy term (Sparrow and Lin, 1964; Minkowycz and Sparrow, 1966; Bejan, 2013). The properties of the gas mixture are assumed to be constant. In addition, the boundary layer hypothesis is adopted. The resulting model is then,

$$\frac{\partial u}{\partial x} + \frac{\partial v}{\partial y} = 0 \tag{21}$$

$$u\frac{\partial u}{\partial x} + v\frac{\partial u}{\partial y} = \nu\frac{\partial^2 u}{\partial y^2} + g\beta_c(W - W_\infty) \tag{22}$$

$$u\frac{\partial W}{\partial x} + v\frac{\partial W}{\partial y} = D_{vg}\frac{\partial^2 W}{\partial y^2} \tag{23}$$

with boundary conditions given by,

$$u(x,\delta) = u_l(x,\delta) = \frac{g\delta^2}{2\nu_l} \tag{24}$$

$$\rho u(x,\delta)\delta'(x) - \rho v(x,\delta) = \dot{m}'' \tag{25}$$

$$u(x, y \to \infty) = 0 \tag{26}$$

$$\dot{m}'' W(x,\delta) + \rho D_{vg}\left(\frac{\partial W}{\partial y}\right)_{y=\delta} = 0 \tag{27}$$

$$W(x, y \to \infty) = W_\infty \tag{28}$$

and,

$$\beta_c = \frac{M_g - M_v}{M_g - (M_g - M_v)W_\infty} \tag{29}$$

where u is the velocity component in the x-direction of the gas mixture, v is the velocity component in the y-direction of the gas mixture, W is the mass fraction of noncondensable gas, ρ is the density of the gas mixture, ν is the kinematic viscosity of the gas mixture, D_{vg} is the diffusivity of vapor in the gas, β_c is the concentration expansion coefficient, W_∞ is the free stream mass fraction of noncondensable gas, M_g is the molar mass of the noncondensable gas, and M_v is the molar mass of the vapor.

The mass fraction of noncondensable gas can be related to the temperature at the interface using the equation of state for ideal gases and Antoine equation (Reid *et al.*, 1977) for the vapor pressure yielding,

$$T_i = \frac{B}{A - \ln\left(\frac{M_g[1 - W(x,\delta)]}{M_g[1 - W(x,\delta)] + M_v W(x,\delta)} p_\infty\right)} - C \tag{30}$$

where p_∞ is the total pressure of the freestream. For T_i in °C and p_∞ in Pa, $A = 23.1964$, $B = 3816.44$, and $C = 227.02$.

2.5 Karman-Pohlhausen integral method

Applying $\int_{\delta(x)}^{\infty} \_ dy$ to eqs. (21-23) and employing the boundary conditions of eqs. (24-28) yields,

$$\frac{d}{dx}\left\{\int_{\delta(x)}^{\infty} u^2 dy\right\} + \frac{\dot{m}''}{\rho} u_l(x,\delta) = -\nu\left(\frac{\partial u}{\partial y}\right)_{y=\delta} + \int_{\delta(x)}^{\infty} g\beta_c (W - W_\infty) dy \tag{31}$$

$$\frac{d}{dx}\left\{\int_{\delta(x)}^{\infty} u(W - W_\infty) dy\right\} = \frac{\dot{m}''}{\rho} W_\infty \tag{32}$$

Approximate profiles are proposed for the velocity component in the x-direction and mass fraction of noncondensable gas. Polynomial functions are prescribed within the boundary layer and constant values are imposed beyond the boundary layer. Polynomials of order 3 and 2 are used for the velocity and mass fraction, respectively. Mathematically,

$$u(x,y) = \begin{cases} f\left(x, \frac{y-\delta}{\delta_v}\right), \delta < y < \delta + \delta_v \\ 0, y > \delta + \delta_v \end{cases} \tag{33}$$

$$W - W_\infty = \begin{cases} \zeta_W\left(x, \frac{y-\delta}{\delta_v}\right), \delta < y < \delta + \delta_v \\ 0, y > \delta + \delta_v \end{cases} \tag{34}$$

with,

$$f\left(x, \frac{y-\delta}{\delta_v}\right) = u_l(x,\delta)\left(1 - \frac{y-\delta}{\delta_v}\right)^2 + u_0(x)\frac{y-\delta}{\delta_v}\left(1 - \frac{y-\delta}{\delta_v}\right)^2 \tag{35}$$

$$\zeta_W\left(x, \frac{y-\delta}{\delta_v}\right) = \frac{W_\infty}{\frac{2\rho D_{vg}}{\dot{m}''\delta_v} - 1}\left(1 - \frac{y-\delta}{\delta_v}\right)^2 \tag{36}$$

where δ_v is the thickness of the momentum and mass fraction boundary layers. Given that, for gas mixtures, $Sc = \nu/D_{vg} \cong 1$, it is assumed in eqs. (33-36) that the boundary layer thickness is approximately the same for momentum and mass fraction. Substituting eqs. (33-36) into eqs. (31,32), differential equations for u_0 and δ_v are obtained.

2.6 Computational procedure

Eqs. (4,5,20,30-32) form a system of differential-algebraic equations to be solved for $T_c(x)$, $\delta(x)$, $T_i(x)$, $u_0(x)$, $\delta_v(x)$. The initial conditions for the boundary layer and film thicknesses are set to be zero at $x = 0$. The function *NDSolve* of the *Wolfram Mathematica v.11.2* (Wolfram, 2017) platform is used for the numerical calculations. In this work, humid air is the gas mixture and liquid water is assumed to flow inside the channel. The thermophysical properties of these materials are taken from the literature (Tsilingiris, 2008; Lide, 2010).

The base case and other materials employed in the analysis are presented in Table 1. Three iterations of solid materials are evaluated further in the text. In addition, different channel width and wall thickness values are used to probe their effect in the heat transfer rate. More specifically, besides the values presented in Table 1, channel widths of 1 and 4 mm, and wall thicknesses of 0.1 and 10 mm are used. These parameters are typical of membrane distillation applications (Shahu and Thombre, 2019).

The total heat transfer rate per unit of depth can be calculated from the heat trespassing the interface between the liquid film and the gas mixture in the following way:

$$Q = \frac{1}{L}\int_0^L \dot{m}'' h_{fg} dx \tag{37}$$

where Q is the total heat transfer rate through the wall per unit of depth. The integration in eq. (37) is carried out numerically with the function *NIntegrate* of the *Wolfram Mathematica v. 11.2* platform (Wolfram, 2017).

On the other hand, the heat transfer rate per unit of depth obtained with the condensation of pure vapor under the Nusselt model can be calculated as (Nusselt, 1916),

$$Q_{Nu} = \frac{4}{3}\mu_l \left[\frac{c_{p,l}\left(T_\infty - T_{c,e}\right)}{Pr_l h_{fg}}\right]^{3/4} \left(\frac{gL^3}{4\nu_l^2}\right)^{1/4} h_{fg} \tag{38}$$

where Q_{Nu} is the heat transfer rate per unit of depth for the Nusselt model, μ_l is the dynamic viscosity of the liquid film, $c_{p,l}$ is the specific heat of the liquid film, and Pr_l is the Prandtl number of the liquid film. The temperature at the entrance of the channel, $T_{c,e}$, is used instead of the constant wall temperature in eq. (38). Therefore, eq. (38) represents a case with the absence of noncondensables, negligible thermal resistance of the wall, and infinite thermal capacity of the fluid flowing along the channel.

Table 1. Entry data for the base case of the analysis and properties of the solid wall for three different materials.

Base case	
Material	Stainless steel
Thermal conductivity (W/mK) (Çengel and Ghajar, 2015)	13.4
Wall thickness (mm)	1
Channel width (mm)	2
Channel flow rate per unit of width (kg/ms)	0.1
Difference between temperatures at the freestream and the entrance of the channel (°C)	20
Channel height (m)	0.1
Bulk gas mixture pressure (bar)	1.014
Other wall materials	
Material	Glass
Thermal conductivity (W/mK) (Çengel and Ghajar, 2015)	0.7
Material	Aluminum
Thermal conductivity (W/mK) (Çengel and Ghajar, 2015)	237

3. RESULTS

In order to verify the model, method, and code developed in this work, an analytical self-similar solution of filmwise condensation with constant wall temperature, T_w (Sparrow and Lin, 1964), is used. The comparison is offered in Fig. 2(a), which presents the mass fraction at the interface as a function of a dimensionless temperature difference between the interface and the wall. Two freestream mass fractions of noncondensable gas are contemplated. Symbols represent the 'exact' similarity solution, while solid lines represent results obtained in this work. The agreement is very good for small temperature differences and marginally good for higher ones. In addition, for higher freestream mass fraction of noncondensable gas, the difference between 'exact' and 'approximate' solutions is less significant due to a steeper mass fraction curve.

To further show the robustness of the proposed approach, Fig. 2(b) presents a comparison with experimental results reported in the literature (Al-Diwany and Rose, 1973) using the fraction of the heat transfer obtained with the Nusselt model (Nusselt, 1916) (Q/Q_{Nu}) as a function of the freestream mass fraction. Solid lines represent results from the present work, while symbols indicate measured values. Two sets of experimental results are available, distinguished from each other by the temperature difference between the wall and the freestream. Squares (orange) and circles (purple) are associated with results for temperature differences below and above 20 K, respectively. As for the numerical calculations from this work, curves for temperature differences of 5, 20, and 80 K are provided. The agreement is very good. The discrepancies observed for lower mass fractions may be attributed of experimental errors, since, in these cases, the heat transfer is more sensitive to inaccuracies in the reported mass fraction (Al Diwany and Rose, 1973).

Overall, verification and validation efforts show that the model and solution methodology are capable of capturing the physics involved in condensation heat transfer in the presence of noncondensable gases, being somewhat more general than previous numerical or analytical works (Sparrow and Lin, 1964; Al-Diwany and Rose, 1973) by including conjugation effects.

Figures 3.(a,b) show the effect of geometrical parameters on the fraction of the heat transfer rate from the classical Nusselt model (Q/Q_{Nu}) attained with conjugation effects in the presence of noncondensable gases, namely wall thickness (Fig. 3.(a)) and channel width (Fig. 3.(b)). Lowering any of these two parameters has the effect of increasing the total heat transfer achieved. The reason is the smaller thermal resistance associated with thinner walls and narrower channels, as expressed by eqs. (3,6).

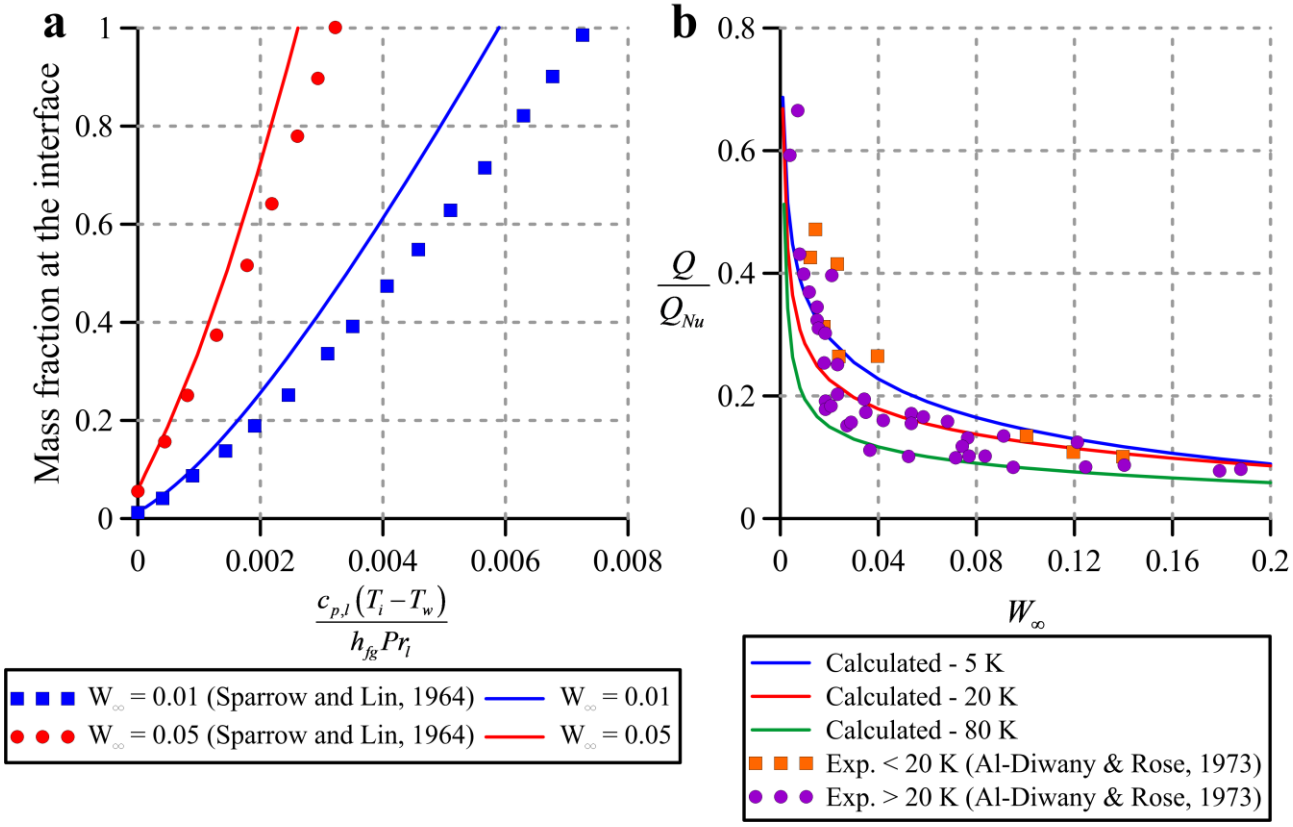

Figure 2. Verification and validation of the model, solution methodology, and code developed. (a) Comparison with 'exact' solution (b) Comparison with experimental results.

Despite the significant reduction in wall thickness compared with the base case (from 1 mm to 0.1 mm), the solid blue line in Fig. 3.(a) does not deviate significantly from the results for t_w = 1 mm. This behavior may be attributed to a dominance of the forced convection in the combined conduction-convection thermal resistance. Such observation is corroborated by the curve associated with a wall thickness equal to 10 mm, which partly diverts the dominance to the heat conduction resistance, thereby markedly reducing the heat transfer rate. Such saturation effect is not observed in the curves associated with different values of channel width shown in Fig. 3.(b), indicating that the thermal resistance associated with forced convection is significantly higher than the one for conduction through the wall in the base case defined by Table 1. In fact, the wall and channel thermal resistances for the base case are 0.746 and 9.11 cm²K/W, respectively; the convection thermal resistance is an order of magnitude higher than the one for conduction.

Moreover, Figs. 3.(a,b) offer a comparison of the results including conjugation effects with an ideal case with negligible wall and channel thermal resistances and a fluid with an infinitely large thermal capacity flowing in the channel, i.e., uniform wall temperature (dashed orange line in Figs. 3.(a,b)). Even in the ideal case, the accumulation of noncondensable gases at the interface between the film and the gas mixture exacts a significant reduction of the heat transfer rate in comparison with the one attained with pure vapor (Nusselt model). The conjugation effects reduce the heat transfer even further, more than halving it in some instances, and underscoring the importance of taking into account the interplay between condensation, conduction, and forced convection.

The effect of the wall material is also probed in Fig. 4. Given the significantly lower thermal conductivity of glass (see Table 1), the heat transfer rate achieved in this case is much smaller than the ones observed for metallic materials. Therefore, the use of glass as the wall material may render the conduction thermal resistance comparable to the forced convection thermal resistance, in the same way as when the wall thickness is raised from 1 mm to 10 mm in Fig. 3.(a). A milder effect is observed when comparing stainless steel and aluminum. Despite the latter having an order of magnitude higher thermal conductivity in comparison with the former (see Table 1), the effect on the heat transfer is negligibly small. The reasons for this saturation are the same as the ones pointed out when varying the wall thickness in Fig. 3.(a); more specifically, the convection thermal resistance is the main limiting factor as far as the heat transfer from the base of the condensate film to the liquid flowing in the channel is concerned. From an application standpoint, in forced-convection-limited situations, it may be pointless to employ a material with exceedingly high thermal conductivity, especially if this option is costly, as it might provide only limited improvements if the objective is to maximize condensation heat transfer rates and, consequently, condensate output.

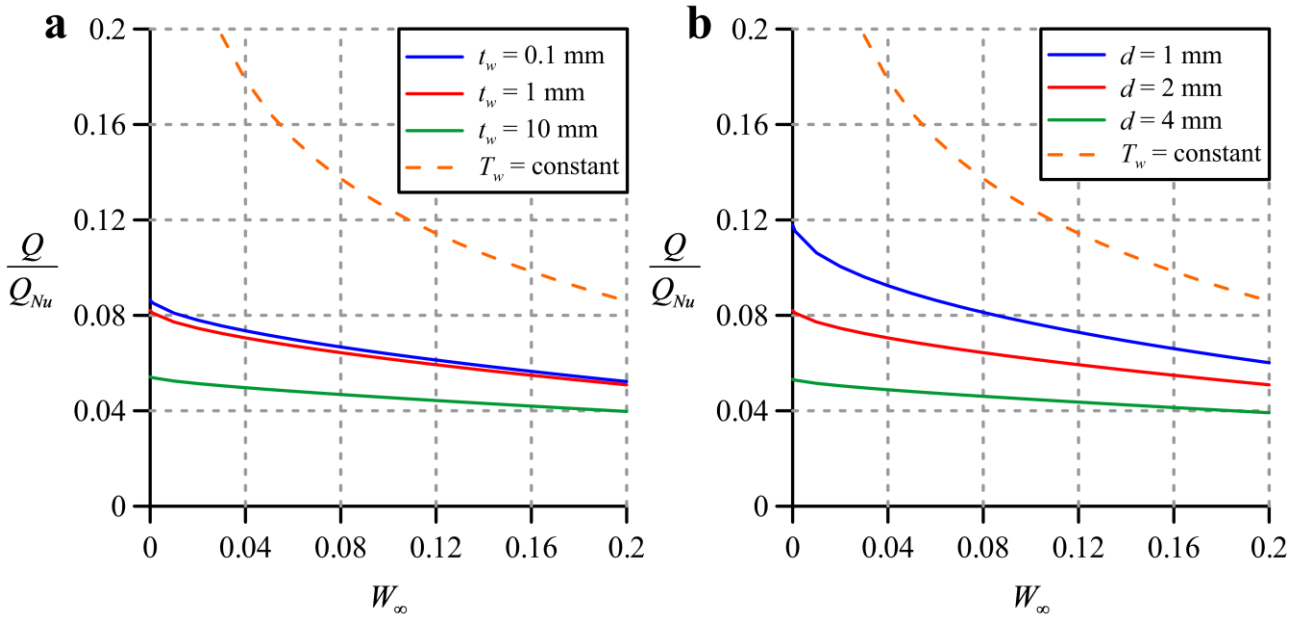

Figure 3. Effects of geometrical parameters in the condensation-conduction-convection conjugated heat transfer. (a) Wall thickness; (b) Channel width. Dashed orange lines represent results for the limiting case of uniform wall temperature.

Once more, in Fig. 4, the conjugate heat transfer results are compared with the limiting case of uniform wall temperature to evaluate the relative importance of taking into account the conduction and forced convection heat transfer phenomena. The added reduction due to conjugate heat transfer effects is very significant, indicating that analyses of systems such as the one illustrated in Fig. 1 must include them to enable accurate results to be attained.

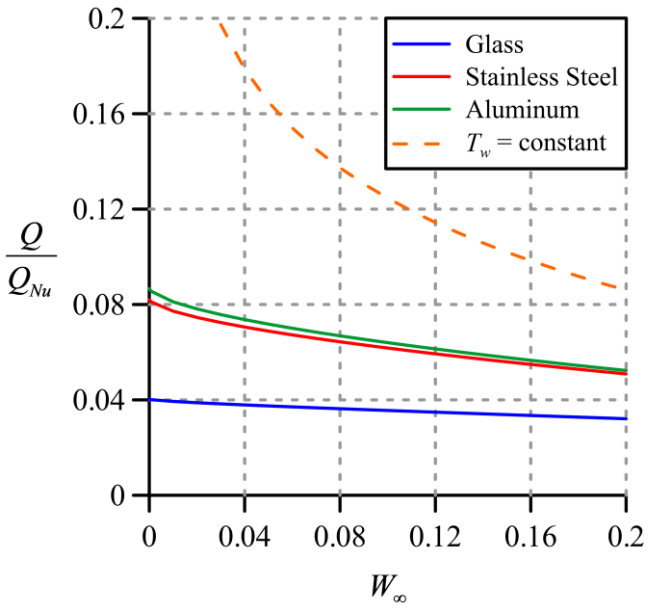

Figure 4. Effect of the wall material in the condensation-conduction-convection conjugated heat transfer. Dashed orange line represents results for the limiting case of uniform wall temperature.

An interesting feature from the results of Figs. 3.(a,b) and (4) is the behavior of the heat transfer rate with increasing mass fraction of the noncondensable gas in the freestream. A steeper decrease is observed for the results without conjugation (uniform wall temperature) in comparison with the ones including conduction through the wall and forced convection in the channel. This behavior is an indication that the conduction and forced convection thermal resistances are able to rival the shielding of vapor from the film-gas mixture interface enacted by the noncondensable gas in the task of reducing heat transfer rates. In fact, in spite of the uniform temperature case tending to the heat transfer rate predicted

by the Nusselt model ($Q/Q_{Nu} \to 1$) as we get closer to having pure vapor, the conjugate heat transfer results present a very limited heat transfer rate, never larger than 12% of the one predicted by the Nusselt model, even at $W_\infty = 0$.

4. CONCLUSION

A theoretical analysis of condensation heat transfer in the presence of a noncondensable gas and involving conjugation effects was carried out. For this purpose, boundary layer models and the Karman-Pohlhausen integral method were employed to solve the governing equations. Favorable comparisons with both previous theoretical and experimental efforts indicate that the adopted approach was able to satisfactorily capture the main phenomena involved.

The analysis showed the importance of taking into account conjugation effects in condensation heat transfer problems, as they may be at least comparable to the presence of noncondensable gases and its severe consequences. The parameters used, typical of desalination applications (Shahu and Thombre, 2019), yielded a forced-convection-limited situation, leading to small improvements in heat transfer rate with reductions in wall thickness and using more conductive wall materials beyond a certain point. These results could be particularly useful in engineering design, since it may not be worth to employ thin foils with high thermal conductivities for only marginal gains in applications where maximizing heat transfer rates is beneficial.

The results of this work can potentially contribute with the evaluation of condensation processes present in far-reaching applications, such as desalination, condensers, heat pipes, nuclear reactors, among others.

5. ACKNOWLEDGEMENTS

The authors are grateful for the financial support offered by the Brazilian Government agencies CNPq, CAPES (PROCAD/DEFESA), and FAPERJ (Grant no. E-26/010/002590/2019).

6. REFERENCES

Al-Diwany, H.K. and Rose, J.W., 1973. “Free convection film condensation of steam in the presence of non-condensing gases”, *Int. J. Heat Mass Transf.*, Vol. 16, No. 7, pp. 1359-1369.

Bejan, A., 2013. *Convection Heat Transfer*, 4th ed., Wiley, New Jersey, NJ.

Çengel, Y.A. and Ghajar, A.J., 2015. *Heat and Mass Transfer: Fundamentals & Applications*, 5th ed., McGraw-Hill, New York, NY.

Collier, J.G. and Thome, J.R., 1994. *Convective Boiling and Condensation*, 4th ed., Oxford University Press, Oxford, UK.

El Fil, B., Kini, G., and Garimella, S., 2020. “A review of dropwise condensation: Theory, modeling, experiments, and applications”, *Int. J. Heat Mass Transf.*, Vol. 160, pp. 120172.

Kandlikar, S.G., Garimella, S., Li, D., Colin, S., and King, M.R., 2006. *Heat Transfer and Fluid Flow in Minichannels and Microchannels*, Elsevier, Oxford, UK.

Lide, D.R., 2010. *Handbook of Chemistry and Physics*, 10th ed., CRC Press, Boca Raton, FL.

Minkowycz, W.J. and Sparrow, E.M., 1966. “Condensation heat transfer in the presence of noncondensables, interfacial resistance, superheating, variable properties, and diffusion”, *Int. J. Heat Mass Transf.*, Vol. 9, No. 10, pp. 1125-1144.

Nusselt, W., 1916. “Die Oberflächenkondensation der Wasserdampfes”, *Z. Ver. Deutsch. Ing.*, Vol. 60, pp. 541-569.

Othmer, D.F., 1929. “The condensation of steam”, *Ind. Eng. Chem. Res.*, Vol. 21, No. 6, pp. 576-583.

Reid, R.C., Prausnitz, J.M., and Sherwood, T.K., 1977. *The Properties of Gases and Liquids*, 3rd ed., McGraw-Hill, NY.

Senjaya, R. and Inoue, T., 2014a. “Effects of non-condensable gas on the performance of oscillating heat pipe, part I: Theoretical study”, *Appl. Therm. Eng.*, Vol. 73, No. 1, pp. 1387-1392.

Senjaya, R. and Inoue, T., 2014b. “Effects of non-condensable gas on the performance of oscillating heat pipe, part II: Experimental study”, *Appl. Therm. Eng.*, Vol. 73, No. 1, pp. 1393-1500.

Shah, R.K. and London, A.L., 1978. *Laminar Flow Forced Convection in Ducts*, *Supplement 1* to *Advances in Heat Transfer*, Academic Press, New York, NY.

Shahu, V.T. and Thombre, S.B., 2019. “Air gap membrane distillation: A review”, *J. Renew. Sust. Energy*, Vol. 11, pp. 045901.

Sharma, C.S., Somatopoulos, C., Suter, R., von Rohr, P.R., and Poulikakos, D., 2018. “Rationally 3D-textured copper surfaces for Laplace pressure imbalance-induced enhancement in dropwise condensation”, *ACS Appl. Mater. Interfaces*, Vol. 10, pp. 29127-29135.

Sparrow, E.M. and Lin, S.H., 1964. “Condensation heat transfer in the presence of a noncondensable gas”, *J. Heat Transfer*, Vol. 86, No. 3, pp. 430-436.

Tsilingiris, P.T., 2008. “Thermophysical and transport properties of humid air at temperature range between 0 and 100 °C”, *Energy Convers. Manag.*, Vol. 49, pp. 1098-1110.

Wolfram, S., 2017. *Wolfram Mathematica 11.2*, Wolfram Research Inc., Champaign, IL.

Zhang, X., Jia, L., Peng, Q., and Dang, C., 2019. “Experimental study of condensation heat transfer in a condenser with a liquid-vapor separator”, *Appl. Therm. Eng.*, Vol. 152, pp. 196-203.